



Investigation on the Properties of Calcium – Sulfate Ultra-Phosphate Glasses Doped Trivalent Samarium: A Potential Use for Radiation Shielding Applications

Aliyu Mohammed Aliyu* and Mohammed Auwal Adamu

¹Nanoscience and Technology Research Group (NSTRG), Department of Physics, Sa'adu Zungur University, Gadau, Bauchi State Nigeria

Corresponding Author: aliyualiyuphy@gmail.com, amaliyu@basug.edu.ng

ABSTRACT

The present study, five different glass samples were encoded as; CSPSm1, CSPSm2, CSPSm3, CSPSm4 and CSPSm5 based on $20\text{CaSO}_4 + (10 - x) \text{P}_2\text{O}_5 - \text{Sm}_2\text{O}_3$, ($0.3 \leq x \leq 1.5$ mol %) were fabricated. XRD spectra verified the amorphous phase of the prepared samples. Phy-X/PSD software was used to ascertain the $\gamma - r$ ray shielding characteristics on ultra-phosphate glasses, this software can generate a data on shielding parameters of a selected energy region between $1.50\text{E} - 02$ to $1.50\text{E} + 01$ with radioactive sources for ^{241}Am , ^{60}Co , ^{109}Cd , ^{137}Cs , ^{152}Eu , ^{55}Fe , ^{131}I , ^{22}Na , and ^{133}Ba with their energies and some K-shell characteristics at the X-ray energies of Ag, Ba, Cu, Rb, Tb and Mo elements. The penetrating ability of such radiations through specific material was discovered. Densities increases simultaneously from 3.145 to 3.987 g/cm^3 , the mass attenuation coefficient depends on sample density, the attenuation coefficient of samples gets enhanced with addition of samarium oxide. Shielding related parameters observed are the Mass attenuation coefficient (MAC), Linear attenuation coefficient (LAC), Half value layer (HVL), Tenth value layer (TVL), Mean free path (MFP), and effective atomic number (Z_{eff}). The attenuation coefficients at 15 keV is between 17.726 and 58.56 cm^{-1} as highest and the lowest at 15 MeV between 0.046 and 0.127 cm^{-1} . The gamma photon energy was evaluated at the range of 0.015MeV to 15 MeV , and the attenuation factors result is highly depended on the concentration of the samarium ion, the material has lower mean free paths. These results proved that the glass samples have excellent gamma-ray shielding effectiveness.

Keywords: Ultra-Phosphate, Gamma rays, X-ray, linear attenuation coefficient, Mass attenuation coefficient, Tenth value layer,

INTRODUCTION

Human beings are exposed to radiation coming from different source this include a cosmic ray, natural radionuclides in water, soil, in air, or plants, and artificial radioactivity from fall-out in nuclear testing and in medical applications. Considering radiation has always occurred in the environment since the earth's origin, daily exposure to various levels of ionizing radiation is in-avoidable for humans, and also, one of the serious problems that may affect human health and the safety on planet is the radiation absorbed or radiation leakage [1]. Due to continuous increase in radiation

absorption on human activities, a suitable shielding on nuclear radiation is highly required to secure life. For such reason, scientists are making efforts to search for shielding materials against nuclear radiation such as gamma rays, X-rays etc. Since excessive exposure to this type of radiation results in negative effects on humans, this may cause serious diseases such as skin burns, cancers, cardiovascular disease, and blood cell damage. At times, long-term exposure to such types of radiation may not only dangerous but could be deadly [1, 2]. This means cancer, cataracts, deterioration of bones, gene mutation, and the possibility of death are the



only a few of the negative impacts. Therefore, several international bodies have found out on standards in relation to radiation hazards which led to the formation of Maximum Permissible Dose (MPL). Meanwhile, it has become necessary to protect humans and their environments from the negative effects of radiation by designing certain types of materials that have the ability to absorb radiation and thus to reduce its impact on humans.

Additionally, radiation shielding was used to protect patients and workers from the exposure of radiation during diagnostic imaging in clinics, hospitals, and/or dental offices. Similar materials are used for other applications such as the scanner curtains used to protect personnel working in the vicinity of airport scanners or any similar devices [3]. Furthermore, radiation shielding glass is a special glass that can protect against such radioactive rays (such as X-rays, γ -rays, etc.) [4]. Lead is the widely-known element used as shielding material, since glasses doped with lead (Pb) are mostly used for radiation shielding application. However, lead oxides possess certain limited characteristic, such as toxicity [5] weak mechanical strength etc. [6,7] this causes many researchers to look for alternative shielding materials, increasing lead oxides concentration may result to decrease in glass hardness, also, is hazardous to the patients and workers that affect the biochemical systems in the human body [8]. The toxicity of lead and other effects encourages several researchers to investigate the lead-free glasses (as a non-toxic material) for radiation shielding target [5, 9]. Thus, Lead (Pb) may be replaced with heavy metals or non-toxic materials are extremely important. Current studies focus the non-toxic material, low chemical abrasion, low cost and flexible shielding material. Investigations on radiation shielding features of various glasses have been

applied for Telluride [10], Silicate [11], Borate [8], Phosphate [9, 10], Barium - Phosphate [11], and Zinc Boro-tellurite [12]. However, Phosphate-based glasses have been developed and investigated in the demands of both industries and for technologies, this is because glass-based exhibits many desirable properties such as low transition temperature, low optical dispersion [13] good applications in optical data transmission [14] good material for laser technologies [15] and serves as a shielding glass [16].

On the other hand, trivalent samarium ion (Sm^{3+}) is among the rare earth ions widely used as an active luminescence material [17] it shows a strong orange to red fluorescence in the visible region [18] it also acts as an acceptor, and can accommodate in the voids associated with PO_4 units of samples network and expands the glass structure results in increase in molar volume [19]. Sm^{3+} doped glasses have attracted much interest due to their applications for visible solid-state lasers, color displays, and high-density optical memory devices [20]. In addition, trivalent samarium can be easily changed to Sm^{2+} with decrease in atmosphere [21], ionizing radiation [22, 23], hence samarium ions are stable in trivalent (Sm^{3+}) as well as divalent (Sm^{2+}) states [24]. Radiation shielding is a boundary placed between a source and a person that needs to be protected against the radiation, mainly to control/limit the radiation exposure rate at a required point. Shielding is based on reduction of strength or energy intensity (attenuation) through a specific medium [25, 26]. The present work reported on gamma-ray shielding factors for calcium ultra-phosphate glasses with chemical compositions of $20\text{CaSO}_4 + (10-x) \text{P}_2\text{O}_5 - \text{Sm}_2\text{O}_3$, ($0.3 \leq x \leq 1.5$ mol %). Many researches have been increased tremendously to investigate on radiation attenuation processes on glass sample using different

methods either by experimental or theoretical method (this is by utilizing simulations) as a computer program as in MCNPX and WinXCOM [27, 28], or Phy-X/PSD [26, 29]. Investigation shows that Phy-X/PSD software is more accurate, faster and more reliable method to find the radiation shielding parameters [30 – 32], this software (Phy-X/PSD) was used to find out the attenuation as well as the penetration ability.

MATERIALS AND METHOD

Glass Synthesis

Radiation shielding properties of glasses with compositions $20\text{CaSO}_4 + (10-x) \text{P}_2\text{O}_5 - \text{Sm}_2\text{O}_3$, ($0.3 \leq x \leq 1.5$) mol %, were investigated using Phy-X/PSD computer program. The composition of sample was

prepared using calcium sulfate (CaSO_4), Phosphoric acid (H_3PO_4), Samarium oxide (Sm_2O_3) in aqueous and powder form. The glasses samples were coded as CSFP:Sm 1 – CSFP:Sm 5 with no variation of CaSO_4 mol % respectively. The compositions of glass and the corresponding densities were listed in Table 1.

RESULTS AND DISCUSSION

Amorphous Characterization

Melt-quenching method was used on Calcium Sulfo-Phosphate glasses with samarium concentrations were prepared. Non-crystalline (amorphous) material were verified and analyzed by X-ray Diffractometer (XRD). Fig. 1 shows where XRD peaks superimposed and broad hump on $2\theta = 18 - 25^\circ$ appeared.

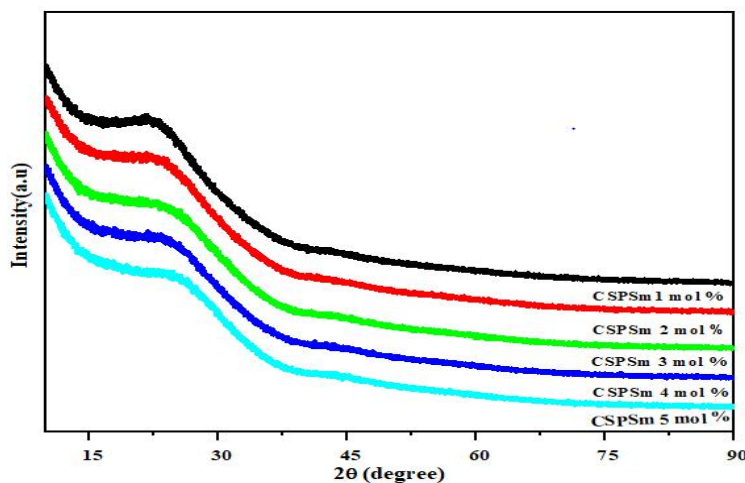


Figure 1: XRD patterns of $20\text{CaSO}_4 + (10-x) \text{P}_2\text{O}_5 - \text{Sm}_2\text{O}_3$, in mol % of glass samples.

Table 1: Shows the composition of $20\text{CaSO}_4 + (10-x) \text{P}_2\text{O}_5 - \text{Sm}_2\text{O}_3$ with $0.3 \leq x \leq 1.5$ mol % glass system and the density (ρ) in g/cm^3 .

Glass acronyms	P_2O_5 mol %	CaSO_4 mol %	Sm_2O_3 mol %	Density
CSP:Sm 1	79.7	20	0.3	3.145
CSP:Sm 2	79.4	20	0.6	3.304
CSP:Sm 3	79.2	20	0.8	3.679
CSP:Sm 4	78.8	20	1.2	3.832
CSP:Sm 5	78.5	20	1.5	3.987

The user-friendly software (Phy-X/PSD) were used to carefully observed the gamma ray shielding characteristics for $20\text{CaSO}_4 + (10-x)$

$\text{P}_2\text{O}_5 - \text{Sm}_2\text{O}_3$ glass systems. This report the penetration and attenuation for the samples at different energies. Some parameters used to

explain the penetrating ability of radiations are; Tenth and Half value layer (*TVL* & *HVL*), Linear and Mass attenuation coefficient (*LAC*, *MAC*), Mean free path (MFP), and the effective atomic number (Z_{eff}). HVL is a measure of radiation shielding effectiveness; it is also used to quantify poly-energetic rays instead of mass and linear attenuation coefficients used for mono-energetic/monochromatic beams, this serve as a surrogate measure of penetrability of an x-ray spectrum (or beam quality). Half value layer shows the low photon energy, thickness of material when the intensity of incoming radiation is reduced by 50% (one-half) is referred to half value layer, and tenth value layer when reduced by one-tenth (10%) these concepts of TVL and HVL are used in shielding design. The rays undergo attenuation primarily by photoelectric effect, Compton scattering and the pair production interactions. Radiation intensity is as a function of thickness (x) of the absorbing material. To come up with shielding effectiveness thus

$$HVL = x_{1/2} = \ln(2)/\mu \text{ (cm)}, \text{ and for } TVL = x_t = \ln(10)/\mu \text{ (4)}$$

For MAC (μ_m) is defined by $\mu_m = \mu/\rho$ (cm)

Where the symbol ρ is the density of the absorbed samples, it's useful because the attenuation is dependent on the density (ρ) of the absorbed material (heavier and the greater number of atoms with regards to photon means more interactions per unit length on materials). Consequently, both HVL and LAC have distinct values for the same materials

LAC is calculated from the intensity formula (I) and is mathematically express as:

$$I = I_0 e^{-\mu x} \text{ (1)}$$

Where I_0 and I are the incidence and transmitted intensities on the material, whereas μ (cm) is linear attenuation coefficient, and x is the thickness of the material, taking the natural log of both sides, the expression became;

$$\ln(I/I_0) = -\mu x \text{ (2)}$$

Eq. (1) may not be valid in case of the broad-beam geometry, the equation turns to buildup factor equation;

$$I = BI_0 \exp^{-\mu x} \text{ (3)}$$

Where B serves a build-up factor or correction factor that is used to correct the beams heterogeneity and the materials absorber thickness. The HVL of absorbed material is defined as the radiation is reduced by one-half, it is designated as;

$$\text{ (4)}$$

$$\text{ (5)}$$

depending on the phase (i.e. solid or liquid phase) and the temperature. Table 2 indicates the few parameters selected and the parameters required for calculations; the selected MAC values for the materials were also tabulated in tables 3. The Table 3 shows the investigated materials for MAC with increasing trends.

Table 2: shows the parameters selected for calculation

S/N	Parameters	Abbreviation	Required parameters
1.	Linear att. co-efficient	LAC	MAC, energy and ρ of materials in g/cm^3
2.	Mass att. co-efficient	MAC	Definition of material and energy
3.	Half value layer	HVL	MAC, energy and ρ of materials in g/cm^3
4.	Tenth value layer	TVL	MAC, energy and ρ of materials in g/cm^3
5.	Mean free path	MFP	MAC, energy and ρ of materials in g/cm^3
6.	Effective atomic number	Z_{eff}	Definition of a materials and energy

Table 3: MAC of $20\text{CaSO}_4 + (10-x)\text{P}_2\text{O}_5 - \text{Sm}_2\text{O}_3$ with $0.3 \leq x \leq 1.5$ mol % glass system obtained by Phy-X/PSD software.

Energy (MeV)	Mass Att. Coefficient (cm^2/g)				
	CSPS1(0.3)	CSPS2(0.6)	CSPS3(0.9)	CSPS4(1.2)	CSPS5(1.5)
1.50E-02	10.264	10.759	11.086	11.735	14.217
2.00E-02	5.640	5.872	6.026	6.331	6.557
3.00E-02	2.213	2.292	2.344	2.448	2.524
4.00E-02	1.612	1.649	1.673	1.721	1.756
5.00E-02	0.485	0.595	0.667	0.811	0.918
6.00E-02	0.352	0.420	0.465	0.555	0.621
8.00E-02	0.238	0.270	0.290	0.332	0.363
1.00E-01	0.192	0.209	0.220	0.243	0.260
1.50E-01	0.147	0.152	0.156	0.163	0.169
2.00E-01	0.128	0.130	0.132	0.135	0.138
2.84E-01	0.110	0.111	0.112	0.113	0.114
3.00E-01	0.108	0.108	0.109	0.110	0.111
3.47E-01	0.101	0.102	0.102	0.103	0.103
4.00E-01	0.095	0.096	0.096	0.096	0.097
5.00E-01	0.087	0.087	0.087	0.087	0.087
6.00E-01	0.080	0.080	0.080	0.080	0.080
6.62E-01	0.077	0.077	0.077	0.077	0.077
8.00E-01	0.070	0.070	0.070	0.070	0.070
8.26E-01	0.069	0.069	0.069	0.069	0.069
1.00E+00	0.063	0.063	0.063	0.063	0.063
1.17E+00	0.058	0.058	0.058	0.058	0.058
1.33E+00	0.055	0.055	0.054	0.054	0.054
1.50E+00	0.051	0.051	0.051	0.051	0.051
2.00E+00	0.044	0.044	0.044	0.044	0.044
2.51E+00	0.039	0.039	0.039	0.039	0.039
3.00E+00	0.036	0.036	0.036	0.036	0.036
4.00E+00	0.032	0.032	0.032	0.032	0.032
5.00E+00	0.029	0.029	0.029	0.029	0.029
6.00E+00	0.027	0.027	0.027	0.027	0.027
8.00E+00	0.024	0.024	0.024	0.025	0.025
1.00E+01	0.023	0.023	0.023	0.023	0.023
1.50E+01	0.021	0.022	0.022	0.022	0.022

The effectiveness of any shielding material is independent of the materials use; this implies that materials for radiation shielding thickness play a significant role also; the density of a

material has a great impact as well. Figure 2a presents linear attenuation coefficient of the samples, as the energy of the photon increases the values of LAC decrease. The materials

were exposed to photon energy from 0.015 MeV (as low photon energy) to 15.00 MeV it's reached the maximum value. The LAC values at minimum photon energy ($E = 0.015$ MeV) are; 17.726 (CSPSm1), 26.38 (CSPSm2), 36.10 (CSPSm3), 46.74 (CSPSm4) and 58.56 cm^{-1} (CSPSm5), respectively and the maximum energy (at 15 MeV) 0.046 (CSPSm1), 0.065 (CSPSm2), 0.086 (CSPSm3), 0.105 (CSPSm4) and 0.127 cm^{-1} (CSPSm5). There is rise in LAC at 0.004 MeV could be as a result of increase in Sm_2O_3 k-absorption edge induced by the photoelectric effect [33, 34]. The maximum and

minimum photon energies indicate the increase as the Sm_2O_3 content rise from 1 to 5 mol%, this result shows that the attenuation factors depend on the concentration of dopant. MAC (as in figure 2b) and values in table 2 of CSPSm1 – CSPSm5 are in the range of $10.264 - 14.217 \text{ cm}^2/\text{g}$ was at lower and higher energies. Photoelectric effect (PE), the pair production (PP) and the Compton scattering (CS) are the interaction process occurred on the materials [35]. The trend of MAC increases with increase in samarium contents as in table 3 which correspond to the increase in density of materials.

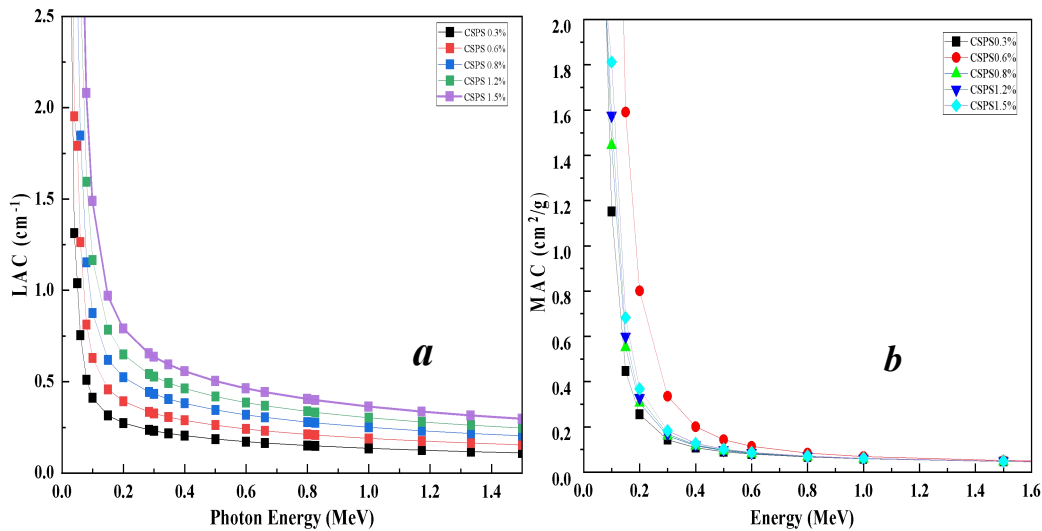


Figure 2: (a & b) LAC and MAC of $20\text{CaSO}_4 + (10-x) \text{P}_2\text{O}_3 - \text{Sm}_2\text{O}_3$ glass systems.

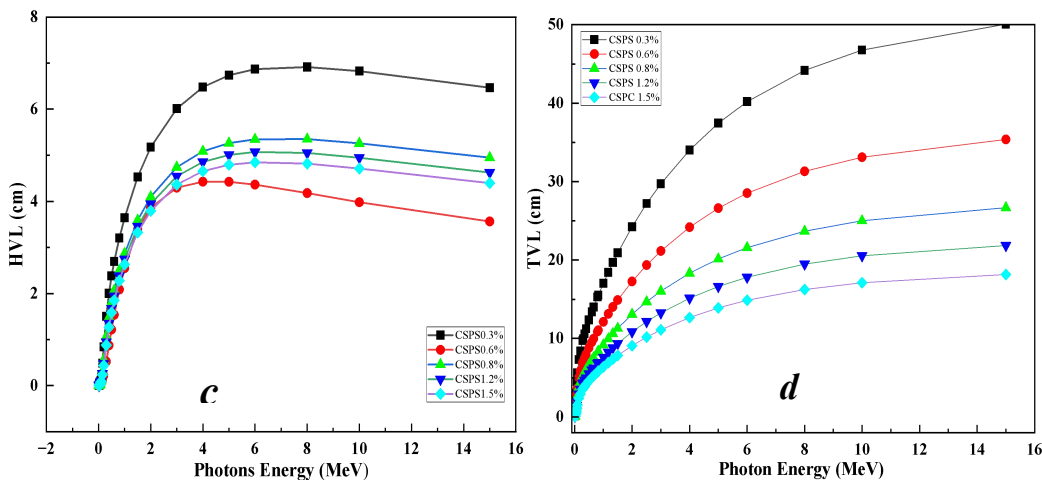


Figure 3: (c & d) HVL and TVL of $20\text{CaSO}_4 + (10-x) \text{P}_2\text{O}_3 - \text{Sm}_2\text{O}_3$ glass systems.

TVL and HVL was described as units of distance either cm or in mm, which are photons energy dependent, and are the most frequently used quantitative raw factor in describing the penetrating ability of radiations through material [36] (as in Figure 3 c and d). The variation in HVL and TVL values for the samples were purely express in terms of the photon interaction, the denser the sample

the lower the values of TVL and HVL, the CSPSm1 shows the lowest HVL and TVL. The higher the density of a glass system minimizes the chances of photon interaction. The sample CSPSm5 (CSPSm1.5%) has the lowest value for HVL and TVL (0.012 and 0.039 cm) at $E = keV$ and when $E = 15 MeV$ the values are 5.467 and 18.160 cm respectively.

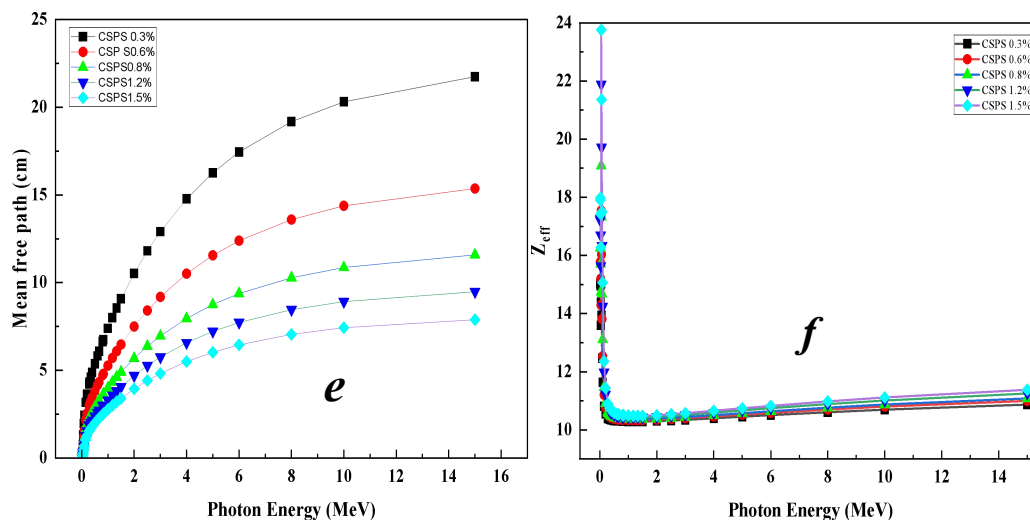


Figure 4: (e & f) MFP and Z_{eff} of $20CaSO_4 + (10-x) P_2O_3 - Sm_2O_3$ glass systems.

MFP also a known as relaxation length (Figure 4e), it emphasizes the superior radiation shielding characteristics and demonstrated the average distance between 2 successive photon interactions. The MFP implies a numerous gamma-ray interaction with the material resulting in higher gamma-ray shielding efficiency. Samples with higher effective atomic number (Z_{eff}) are considered as good candidates for gamma radiation shielding. The attenuation of photons is highly dependent on Z_{eff} as observed by [13, 37]. Meanwhile, materials with higher affective atomic number have larger targets for photons to collide with atoms/ions in the material, hence the interaction is high. Materials with high-reaching Z_{eff} the photons attenuation were relatively high. In most practical applications, higher effective atomic number

glasses are recommended and suitable for protection from γ -radiation. Phy-X/ PSD program was used to compute the Z_{eff} of the $20CaSO_4 + (10-x) P_2O_3 - Sm_2O_3$ glass samples (see Fig. 4f). Same results were verified in $TeO_2-B_2O_3-SiO_2$ glass doped Bi_2O_3 using Phy-X/PSD software [35] and γ -ray shielding characteristics of $CaF_2-BaO-P_2O_5$ [17, 29] glasses. The figure presents the Z_{eff} as a function of photon energy for CSPS1 – CSPS5 glasses. The values of Z_{eff} occur for 15keV to 15MeV are 15.02, 15.77, 16.26, 17.21, and 17.90 and 10.87, 11.00, 11.08, 11.26, and 11.38 for CSPS1 – CSP5 respectively. The values show a slow increment were the CS process is dominant. Furthermore, the effective atomic number values become constant for the energy above 12megelectron volt (MeV) this ascribes to



dominance of pair production. Therefore, Z_{eff} depends on the concentration of trivalent samarium oxides; it increases with increasing trivalent samarium oxide from 15.02 to 17.21 at photon energy 15 keV.

CONCLUSION

Glass composition $20\text{CaSO}_4 + (10-x)\text{P}_2\text{O}_5 - \text{Sm}_2\text{O}_3$ was prepared using melt quenching techniques, XRD analysis indicates no peaks, this shows the materials is in amorphous state. Samarium doped attracts much attention due to their applications for visible solid-state lasers, color displays, and high-density optical memory devices. This glass was prepared for gamma ray shielding applications. The results reveal the improvement on network stability and the chemical durability with increasing modifier oxides as well as the dopant. Phy-X/PSD software was used to interpret the γ - r ay shielding properties ultra-phosphate glasses. The LAC values at minimum photon energy ($E = 0.015$ MeV) are; 17.726 (CSPSm1), 26.38 (CSPSm2), 36.10 (CSPSm3), 46.74 (CSPSm4) and 58.56 cm^{-1} (CSPSm5), respectively and the maximum energy (at 15 MeV) 0.046(CSPSm1), 0.065 (CSPSm2), 0.086 (CSPSm3), 0.105 (CSPSm4) and 0.127 cm^{-1} (CSPSm5). Attenuation factors are highly dependent on Sm_2O_3 content, the software generate a data on MAC, HVL, LAC, TVL, MFP, and effective atomic number (Z_{eff}) in a wide energy ranges, the attenuation coefficients at 15 keV (between 17.726 and 58.56 cm^{-1}) as highest and the lowest at 15 MeV (between 0.046 and 0.127 cm^{-1}). Gamma photon energy was evaluated at the range of 0.015MeV to 15 MeV, and attenuation factors result is highly depended on the concentration of the samarium ion, the material has lower mean free paths. These results proved that the glass samples have excellent gamma-ray shielding effectiveness. An important feature of this software is that it can calculate/compute all shielding parameters

simultaneously, very fast and accurate way, also, user is having alternative to select the desired parameters from all indicated shielding parameters and save the data in an Excel file designed in an understandable, logical and a practical form. The accuracy of the program was checked by comparing values with those in literature. The program helped and developed low cost and reliable shielding materials in finding accurate calculations. Finally, the samples of doped samarium oxide serve as a new lead-free gamma ray shielding material.

Acknowledgement

We are grateful to Tertiary Education Trust Fund (TETFund) for their support and financing the research under the year 2023 TETFUND INTERVENTION IN RESEARCH PROJECT (RP): DISBURSEMENT OF FIRST TRANCH OF FUNDS (BASUG/CERI/IBR/023/Vol.1).

REFERENCES

- [1] Nadn J. A., Noorfatin A B-Amin., Rafidah Z. (2019). Conventional and new lead-free radiation shielding materials for radiation protection in nuclear medicine: A review: *Radiation Physics and Chemistry*, 165, 108439
- [2] M. Hammam, E. Kilany, E. Nabhan, A. Abdel Moghny, A. Atta, (2022), Physical, Optical and Radiation Shielding Properties of Some Phosphate Glasses, *Egyptian Journal of Chemistry*, 65 (8), 499 – 509
- [3] McCaffrey J. P., Shen H., Downton B., and Mainegra-Hing E. (2007). Radiation attenuation by lead and non-lead materials used in radiation shielding garments, *Med. Phys.* 34 (2) 530 – 537.
- [4] Dahindeal P. S, Dapkeb G. P, Rautc S.D, Bhosaled R. R, and Pawar P. P, (2019) Analysis of Half Value Layer (HVL), Tenth Value Layer (TVL) and Mean Free Path (MPF) of some oxides in the energy range of 122 keV to 1330keV *Indian Journal of Science Research* 09 (2): 79-84.



- [5] Vadavathi, A. M., Chinthakayala, S. K., Kollipara, V. S., Ramadurai, G., & Gadige, P. (2021) Physical properties and gamma radiation shielding capability of highly dense binary bismuth borate glasses, *Ceramics International*, 47(7), 9791–9805
- [6] Erdem Ş., Özgür F. Ö, Bünyamin A., Sayyed M. I., Murat K., (2020), Phy-X / PSD: Development of a user-friendly online software for calculation of parameters relevant to radiation shielding and dosimetry, *Radiation Physics and Chemistry* 166, 108496 1 – 12
- [7] Soylu H. M, Lambrecht F. Y, Erso O, A (2015) Gamma radiation shielding efficiency of a new lead-free composite material, *Journal of Radioanal Nucl Chem* 305:529 –534
- [8] Hsiao, C., Wu, K., Wan, K. (2011). Effects of environmental lead exposure on T-helper cell-specific cytokines in children. *J. Immunotoxicology*. 8 (10), 284 –287
- [9] Sayyed M. I. (2016). Bismuth modified shielding properties of Zinc Boro-Tellurite glasses. *J Alloys Compd*, 688,111–117
- [10] El-Mallawany R., Sayyed M. I., Dong M. G., (2017). Comparative shielding properties of some tellurite glasses: Part 2. *Journal of Non-Cryst Solids*, 474,16 – 23
- [11] Chanthima N., Kaewkhao J., Limsuwan P. (2012) Study of photon interactions and shielding properties of silicate glasses containing Bi₂O₃, BaO and PbO in the energy region of 1keV to 100 GeV. *Ann Nucl Energy*, 41,119 –24.
- [12] Saeed A., Elbasha Y. H., El-Shazly R. M. (2016). Optical properties of high-density barium borate glass for gamma ray shielding applications. *Opt Quantum Electron*, 48 (1) 1–10
- [13] Kaewkhao J, Limsuwan, P. (2010) Mass attenuation coefficients and effective atomic numbers in phosphate glass containing Bi₂O₃, PbO and BaO at 662 keV, *Nuclear Instruments and Methods in Physics Research A* 295–297
- [14] Aliyu M. A, Rosli H, Ahmad N. E, Yamusa Y. A (2018) Samarium doped calcium sulfate ultra- phosphate glasses: Structural, physical and luminescence investigations, *International Journal of Light and Electron Optics* 1162 – 1171
- [15] Abdi M. I., El-Ati, A, A. Higazy, (2000), Electrical conductivity and optical properties of gamma- irradiated niobium phosphate glasses, *J. Mater. Sci.* 35 (2) 6175 – 6180
- [16] Agar O., Khattari Z, Y, Sayyed M. I, Tekin H. O., Al-Omari S, Maghrabi., Zaid M. H.M, Kityk, I. V (2019), Evaluation of the shielding parameters of alkaline earth-based phosphate glasses using MCNPX code. *Results Phys.* 12, 101–106
- [17] Mierzejewski A., Saunders G. A., Sidek H. A. A., Bridge B., (1988), Vibrational Properties of Samarium Phosphate Glasses, *Journal of Non-Crystalline Solids* 104 (5) 323-332
- [18] Nachimuthu P, Jagannathan R, Nirmal Kumar V., Narayana Rao D (1997) Absorption and emission spectral studies of Sm³⁺ and Dy³⁺ ions in PbO-PbF₂ glasses, *J. of Non-Crystalline Solids* 217 (9) 215-223
- [19] Mierzejewski A, Saunders G. A, Sidek H. A.A, Bridge B, (1988) Vibrational properties of samarium phosphate glasses, *Journal of Non-Crystalline Solids* 104 (2-3) 323 – 332
- [20] Seshadri M, Radha M, Rajesh D, Barbosa L. C, Cordeiro C. M. B, Ratnakaram Y. C, (2015), Effect of ZnO on spectroscopic properties of Sm³⁺ doped zinc phosphate glasses, *Physica B* 459 (2015) 79 – 87
- [21] Song H, Hayakawa T, Nogami M, (1999), Room temperature spectral hole burning and electron transfer in Sm-doped aluminosilicate glasses *J. Appl. Phy.* 86 (9) 5619
- [22] Malchukova E, Boizot B, Petite G, Ghaleb D, (2007) Optical properties and valence state of Sm ions in aluminoborosilicate glass under β-irradiation, *J. Non-Cryst. Solids* 353 (6) 2397
- [23] Abouhaswa A. S, Sayyed M. I, Abeer., Altowyan S, Al-Hadeethi Y, Mahmoud K. A., (2020), Synthesis, optical and radiation



- shielding capacity of the Sm_2O_3 doped borate glasses, *J. Non-Cryst. Solid* (Article in press)
- [24] Chuanxiang Q, Yanlin H, Wanxue Z, Liang S, Hyo Jin S., (2010), Luminescence spectroscopy and crystallographic sites of Sm^{2+} doped in $\text{Sr}_6\text{BP}_5\text{O}_{20}$, *Materials Chemistry and Physics* 121 (2010) 286–290
- [25] Al-Hadeeth Y, Sayyed M. I., (2020) Evaluation of gamma ray shielding characteristics of $\text{CaF}_2\text{-BaO-P}_2\text{O}_5$ glass system using Phy-X / PSD computer program, *Progress in Nuclear Energy* 126 (3) 1 – 6
- [26] Dong M. G., El- Mallawany, R., Sayyed M. I, Tekin H. O, (2017) Shielding properties of $80\text{TeO}_2\text{-}5\text{TiO}_2\text{-}(15-x)\text{WO}_3\text{-}x\text{AnOm}$ glasses using WinXCom and MCNPS code *Radiat. Phys Chem* 141: 172 – 178.
- [27] Sayyed M I., Elbashir B. O., Tekin H. O., Altunsoy E. E., Gaikwad D. K., (2018) Radiation Shielding properties of pentatenary borate glasses using MCNPX code *Journal of Phys. Chem Solid* 12117 – 21.
- [28] Al-hadeethi Y., Sayyed M. I., (2000) A comprehensive study on the effect of TeO_2 on the radiation shielding properties of $\text{TeO}_2\text{-Bi}_2\text{O}_3\text{-LiF-SrCl}_2$ glass system using Phy-X/PSD software. *Ceram Int* 46: 6136 – 6140
- [29] Sakar E., Ozpolat O. F., Ahm B., Sayyed M. I., Kurudirek M., (2020) Phy-X/PSD: Development of user-friendly online software for calculation of parameters relevant to radiation shielding dosimetry. *Rad Phy Chem.* 166: 108496
- [30] Askin A., (2020) Evaluation of the radiation shielding capabilities of the $\text{Na}_2\text{B}_4\text{O}_7\text{-SiO}_2\text{-MoO}_3\text{-Dy}_2\text{O}_3$ glass quaternary using Geant4 simulation code and Phy-X/PSD database. *Ceram Int* 46: 9096 – 102
- [31] Saadu Y. I., Albaqami M. D., Saikh M., Mayeen U. K, Mohammad M. R, Rajesh H., Khalid H. M, (2024) Investigation on radiation shielding potentials of barium calcium aluminosilicate glass material using silicon carbide nanotubes reinforcement. *Radiation Physics and Chemistry* 225: 112158
- [32] Gaafar M. S., Marzouk, S. Y., Mahmoud, I, S., El-Aziz, A. M. A., and Afifi, M (2020), Influence of Samarium on some acoustical, physical and radiation shielding characteristics of $\text{Bi}_2\text{O}_3\text{-ZnO-PbO}$ glasses, *Journal of Material Science: Materials in Electronics*, 31(23), 21502 – 21514
- [33] Saudi, H, A., Halima, M, K., Muhammad, F, D., and Chan, K, T., (2019) Structural and Optical properties of Samarium oxide Zinc Telluride Glass System Doped with Silver Oxide, *Journal of Solid State Science and Technology Letters.*, 20 (4) 13 – 17
- [34] Geidam I. G, Matori K A, Halimah K. M, Chan, K. T, Muhammad F. D, Ishak M, Umar, S. A (2022) Oxide ion Polarizability and gamma radiation shielding features of $\text{TeO}_2\text{-B}_2\text{O}_3\text{-SiO}_2$ glasses containing Bi_2O_3 using Phy-X/PSD software, *Materials Today Communications* 31(7) 103472
- [35] Kharita M.H., Jabra R., Yousef S., Samaan T. (2012). Shielding properties of lead and barium phosphate glasses, *Radiat Phys Chem*, 81 (5) 1568–71
- [36] Sabah M. A., (2013), Investigation the Effective atomic number, electron density, half value layer and mean free path of steel types 304 and 307 in the energy range 40KeV-130KeV, *Journal of Natural Sciences Research*, 3 (15) 107 – 117
- [37] El- Bashir, B. O., Sayyed, M. I., Zaid, M. H. M., & Matori, K. A. (2017) Comprehensive study on physical, elastic and shielding properties of ternary $\text{BaO-Bi}_2\text{O}_3\text{-P}_2\text{O}_5$ glasses as a potent radiation shielding material. *Journal of Non-Crystalline Solids*, 468 (4) 92 – 99.